Electronic Supplementary Material (ESI) for Environmental Science: Processes & Impacts.

Supporting information

Preferential adsorption and coprecipitation of permafrost organic matter with poorly crystalline iron minerals

Eva Voggenreiter[1], Philippe Schmitt-Kopplin[2,3], Laurel ThomasArrigo[4], Casey Bryce[5], Andreas Kappler[1,6], Prachi Joshi[1,]*

[1] Geomicrobiology, Department of Geosciences, University of Tübingen, Schnarrenbergstrasse 94-96, 72076 Tübingen, Germany

[2]Analytical Biogeochemistry, Helmholtz Center Munich, Ingolstädter Landstrasse 1, 85764 Neuherberg, Germany

[3]Analytical Food Chemistry, Technical University of Munich, Maximus-von-Imhof-Forum 2, 85354 Freising

[4]Environmental Chemistry, University of Neuchâtel, Avenue de Bellevaux 51, CH-2000, Neuchâtel, Switzerland

[5]School of Earth Sciences, University of Bristol, Wills Memorial Building, Queens Road Bristol BS8 1RJ, United Kingdom

[6]Cluster of Excellence: EXC 2124: Controlling Microbes to Fight Infection, Schnarrenbergstrasse 94-96, 72076 Tübingen, Germany

Table of Contents

Supplementary Methods:

Text S1: Ferrihydrite characterization

^{57}Fe Mössbauer spectroscopy was used to confirm mineral identity. Samples were inserted into a closed-cycle exchange gas cryostat (Janis cryogenics) under a backflow of He. Spectra were collected at 6 K using a constant acceleration drive system (WissEL) in transmission mode with a ^{57}Co/Rh source. All spectra were calibrated against an α-^{57}Fe foil that was measured at room temperature. Data analysis was performed using Recoil (University of Ottawa) and the extended Voigt Based Fitting routine[1]. The half width at half maximum was constrained to 0.138 mm s^{-1} during fitting.

Specific surface area was determined by Micromeritics Gemini VII surface area and porosity analyzer (Micromeritics Instrument Corporation, USA) on freeze-dried aliquots. For surface area analysis, freeze-dried samples were outgassed with N_2 for 24 h at 298 K to avoid mineral transformation[2] and N_2 adsorption was quantified at 77 K at partial pressure ranges from 0.05 to 0.3 p/p_0. Specific surface area was determined by the BET (Brunauer-Emmett-Teller) equation[3].

Text S2: Calculation of bound organic carbon amount and Langmuir isotherm fitting

To calculate the mass of OC bound to ferrihydrite, the dissolved OC concentration remaining in solution after adsorption (equilibrium DOC) was subtracted from the initial dissolved OC concentration of each dilution and normalized to the measured ferrihydrite content. The DOC concentration in WEOM-free control was used for blank correction. The mass of bound OC in all the adsorption experiments was used to create Langmuir isotherms which enable to calculate the maximum adsorption capacity (q_{max}) of each WEOM type to ferrihydrite[4]:

$$\mathbf{q = q_{max} \frac{K_L \times c_{eq}}{1 + K_L \times c_{eq}}} \quad \textbf{(1)}$$

The variable q stands for the amount of adsorbed OC [mg OC g^{-1} Fh], K_L is the sorption coefficient [L mg^{-1} C] and c_{eq} is the equilibrium concentration of DOC in the aqueous phase [mg C L^{-1}]. Best fit parameters of K_L and q_{max} were obtained by minimizing the square difference of the q values based on experimental data and the initial model. A 95% confidence interval was calculated to assess the uncertainty of the model fit.

Text S3: Fe *K*-edge X-ray absorption spectroscopy (XAS)

Data processing included energy calibration of all sample spectra to the reference foil, pre-edge subtraction and post-edge normalization, as well as adjustment of the edge energy of each spectrum to the zero-crossing of the second-derivative of the X-ray absorption near-edge structure (XANES) region using Athena[5]. Linear combination fitting (LCF) of the XANES

spectra was done from -20 to 30 eV (around the edge energy) with ferrihydrite and Fe(II)-citrate as references to determine Fe oxidation state. Fe speciation was determined by LCF of the k^3-weighted extended X-ray absorption fine structure (EXAFS) spectra in a *k* range from 2 to 11 $Å^{-1}$. The following references were included: ferrihydrite, lepidocrocite, Fe(III)-citrate and Fe(III)-catechol. The edge energy of all spectra and reference samples was set to 7128 eV. Components were constrained between 0 and 100% during LCF fitting, but no constraints were set for the sum of all components. Initial fractions of detected Fe phases were re-calculated to sum up to 100%. The Fe binding environment was further determined by shell fitting, using Artemis[5]. Therefore, the k^3-weighted EXAFS spectra were Fourier-transformed in a *k*-range from 2 to 12 $Å^{-1}$ using the Kaiser-Bessel window function, width of 3 $Å^{-1}$ and Rbkg of 1. Theoretical phase-shift and amplitude functions were calculated with FEFF v.6 based on the structure of goethite[6].

Text S4: Fourier-transform ion-cyclotron-resonance mass spectrometry (FT-ICR-MS)

Samples were injected undiluted into the electrospray chamber at 120 µL/h by a syringe pump. 500 scans were averaged per sample and spectra were internally calibrated using well-known constituents of NOM spanning m/z ratios from 255 to 949 with a mass error less than 0.5 ppm. Data processing was done using Compass Data Analysis (Bruker, Bremen, Germany) and formula assignment of peaks with a signal to noise ratio higher than 4 was performed by an in-house software of the Research Unit Analytical Biogeochemistry (Helmholtz Center Munich). Recovery of the solid phase extraction was checked by drying methanol extracts under constant N_2 flow. Samples were re-dissolved with DDI water and dissolved OC concentration was measured by a TOC analyzer (multi N/C 2100S, Analytik Jena AG, Germany). Recovery was 84 ± 28%. It is known that SPE has a bias towards specific OC classes but we assume that this bias is similar for samples before and after binding for each WEOM type.

Overview of sampling points

Figure S1: Map of Stordalen Mire (Abisko, Sweden) with marked sampling points. Abbreviation OH stands for organic horizon (used for water extracts). Image from Google Earth, taken in August 2022.

Experiment conditions

Table S1: Overview of conducted adsorption and coprecipitation experiments, including the initial OC concentration in WEOM, pH of the experiment, resulting maximum OC binding capacity (q_{max}) and goodness of fit (R^2).

Experiment	thaw stage	Initial OC [mg C/L]	pH	q_{max} [mg C/ g Fh][a]	q_{max} [mg C/g Fe]	R^2
Adsorption with ferrihydrite	Palsa	17.9	4.5	204	391[b]	0.96
	Bog	9.81	4.5	226	433[b]	0.80
	Fen	12.7	6.0	80.9	155[b]	0.78
Coprecipitation with dissolved Fe(II)	Palsa	16.4	4.5		925[c]	n.a.
	Bog	23.5	4.5		1532[c]	n.a.

[a]: estimated via Langmuir fitting, [b]: re-calculated per g Fe for adsorption experiments, [c]: based on highest measured C:Fe ratio in solid by coprecipitation

Table S2: Parameters of adsorption experiments including specific surface area (SSA) of ferrihydrite, initial molar C:Fe ratios in solution, added ferrihydrite concentrations and resulting mean bound OC content.

thaw stage	SSA of added ferrihydrite [m^2/g]	initial C:Fe ratio [mol/mol]	added ferrihydrite [mg/L]	bound OC [mg C/g Fh]
Palsa	195	0.5	80.0	60.7
		0.8	80.0	93.3
		1.0	80.0	134.1
		1.2	80.0	140.7
		1.6	80.0	151.7
		1.9	80.0	182.4
		2.0	80.0	197.2
		2.1	80.0	193.2
		3.3	50.0[1]	199.1
Bog	203	0.5	50.0	58.7
		0.9	50.0	75.3
		1.1	50.0	121.1
		1.3	50.0	107.7
		1.6	50.0	134.0
		1.7	50.0	149.8
		1.8	50.0	148.0
		2.5	40.0[1]	161.0
Fen	195	0.5	70.0	37.92
		0.7	70.0	44.92
		1.0	70.0	57.10
		1.1	70.0	84.03
		1.4	70.0	76.01
		1.7	70.0	77.71
		1.8	70.0	70.24

[1]: Ferrihydrite concentrations were decreased to attempt to reach the saturation threshold and better constrain the Langmuir fit.

Percentage of precipitated Fe and OC during coprecipitation

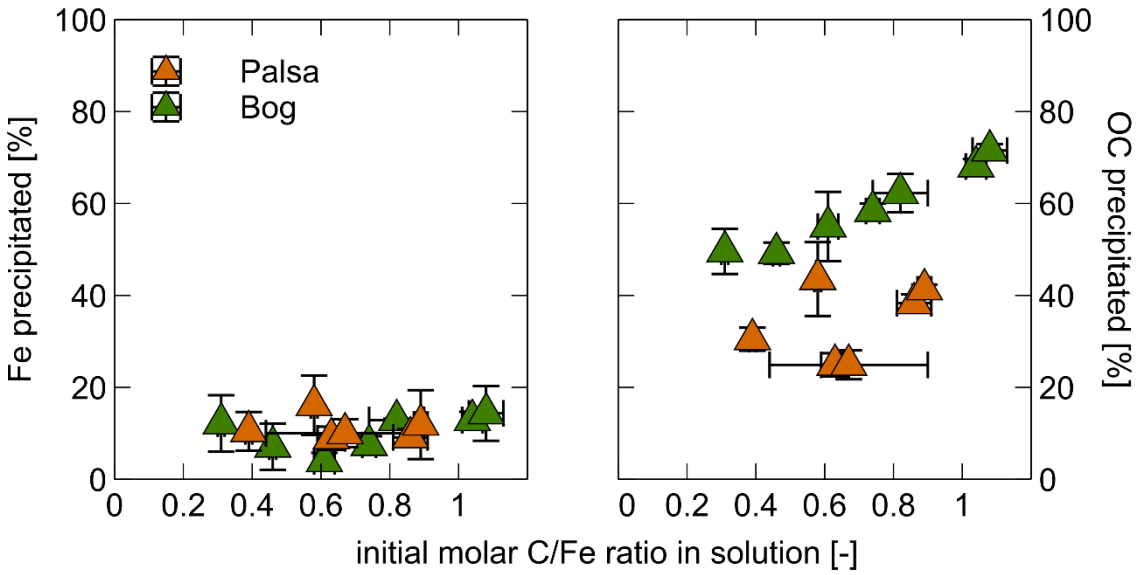

Figure S2: Percentage of precipitated Fe (left) and organic carbon (right) from WEOM of palsa and bog soils by coprecipitation as function of the initial molar C/Fe ratio [mol/mol]. All data points and error bars represent the average and standard deviation of experimental triplicates.

Comparison of C:Fe ratios to other published values

Table S3: Maximum organic carbon to iron weight ratios (C:Fe) of formed Fe-OC associations with organic carbon from palsa, bog and fen soils in adsorption and coprecipitation laboratory experiments (this study) compared to field-based studies. Ratios represent previously published values of ferrihydrite-coated sand that was exposed over 2 months in permafrost soils (estimating adsorption potentials) and average ± standard deviation of dithionite-citrate-bicarbonate (DCB) extractions from soil cores across different sites (indicative of OC bound by coprecipitation).

	C:Fe [g/g]			
	adsorption	coprecipitation	ferrihydrite sand[1] (Stordalen Mire)	DCB extractions (Stordalen Mire)[2,3]
Palsa	0.39 ± 0.04	0.93 ± 0.4		8.7 ± 3.6
Bog	0.44 ± 0.01	1.53 ± 0.9	0.28	7.3 ± 5.1
Fen	0.16 ± 0.01		0.73	0.0 ± 0.0

[1]Patzner et al, 2022a
[2]Patzner et al., 2020
[3]Patzner et al., 2022b

Cation concentrations in WEOM

Table S4: Cation concentrations measured in the initial WEOM of each thaw stage, used for adsorption (ads) and coprecipitation (cop) experiments. Measurements were done using inductively coupled plasma mass spectrometry (ICP-MS, Agilent 7900, Agilent Technologies, USA) with Ar as carrier gas and in He mode for Al, K, Ca and no-gas mode for Mg.

WEOM	Mg [µM]	Al [µM]	K [µM]	Ca [µM]
Palsa_ads	0.6	1.3	2.5	3.5
Bog_ads	0.0	0.6	1.0	3.1
Fen_ads	0.0	0.3	7.4	0.1
Palsa_cop	0.0	0.2	4.1	1.5
Bog_cop	0.4	0.5	1.3	5.4

XAS spectra and fitting

XANES spectra and fitting

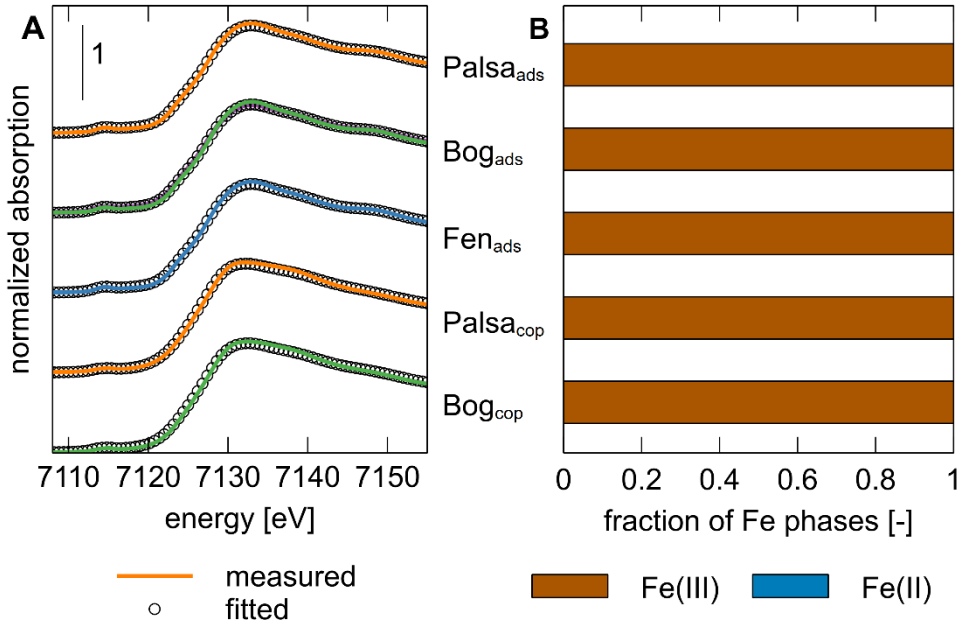

Figure S3: Linear combination fitting of Fe *K*-edge X-ray absorption near edge structure spectra of ferrihydrite with adsorbed WEOM (ads) of palsa, bog and fen soils, and Fe-OC coprecipitates (cop) synthesized with WEOM from palsa and bog soils (A). Speciation of Fe in Fe-OC associations. The same labelling as for graph (A) applies. All Fe was Fe(III) (B). Ferrihydrite and Fe(II)-citrate were used as reference spectra for Fe(III) and Fe(II), respectively.

Table S5: Linear combination fit results for Fe K-edge XANES spectra of ferrihydrite with adsorbed WEOM (ads) of palsa, bog and fen, and Fe-OC coprecipitates (cop) synthesized with WEOM from palsa and bog soils. Ferrihydrite and Fe(II)-citrate were used as reference spectra for Fe(III) and Fe(II), respectively.

sample	Fe(III) [%]	Fe(II) [%]	NSSR[a] [%]	red. $X^{2,b}$ [%]
Palsa_ads	100	0	0.05	0.01
Bog_ads	100	0	0.10	0.02
Fen_ads	100	0	0.06	0.02
Palsa_cop	100	0	0.10	0.10
Bog_cop	100	0	0.15	0.15

[a] normalized sum of of squared residuals (residuals ($100 \sum_i (data_i\text{-}fit_i)^2/\sum_i data^2$)

[b] measure of fit accuracy ($((N_{idp}/N_{pts}) \sum_i ((data_i\text{-}fit_i)/\varepsilon_i)^2(N_{idp}\text{-}N_{var})^{-1})$,). N_{idp}/N_{pts} and N_{var} are the number of independent points in the model fit (37.5), the total number of data points (250) and the number of fit variables (2), respectively.

EXAFS linear combination fitting results

Table S6: Linear combination fit results for Fe *K*-edge EXAFS spectra of ferrihydrite with adsorbed WEOM (ads) of palsa, bog and fen, and Fe-OC coprecipitates (cop) synthesized with WEOM from palsa and bog soils.

sample	ferrihydrite [%]	lepidocrocite [%]	Fe(III)-OM [%]	NSSR[a] [%]	red. $X^{2,b}$ [-]
Palsa_ads	95	5	0	3.0	0.08
Bog_ads	92	8	0	2.7	0.20
Fen_ads	91	9	0	2.5	0.07
Palsa_cop	63	0	37	6.0	0.10
Bog_cop	64	0	36	1.6	0.28

[a] normalized sum of of squared residuals (residuals ($100 \sum_i (data_i\text{-}fit_i)^2/\sum_i data^2$)

[b] measure of fit accuracy ($((N_{idp}/N_{pts}) \sum_i ((data_i\text{-}fit_i)/\varepsilon_i)^2(N_{idp}\text{-}N_{var})^{-1})$,). N_{idp}/N_{pts} and N_{var} are the number of independent points in the model fit (18.2), the total number of data points (181) and the number of fit variables (2-4), respectively.

Shell fit parameters and spectra

Table S7: Shell-fit parameters determined from Fourier-transformed Fe *K*-edge EXAFS spectra of ferrihydrite with adsorbed WEOM (ads) of palsa, bog and fen, and Fe-OC coprecipitates (cop) synthesized with WEOM from palsa and bog soils.

sample	ΔE_0[a] [eV]	Fe-O			Fe-Fe_1			Fe-Fe_2			NSSR[e] [%]	red. $X^{2,f}$
		CN[b]	R[c] [Å]	$\sigma^{2,d}$	CN	R [Å]	σ^2	CN	R [Å]	σ^2		
$Palsa_{ads}$	-5.12 ± 1.78	5.5	1.97	0.012	2.1	3.03	0.012	1.9	3.44	0.008	2.0	468
Bog_{ads}	-3.07 ± 1.27	5.4	1.98	0.011	2.5	3.05	0.012	1.9	3.45	0.008	1.1	516
Fen_{ads}	-3.18 ± 1.15	4.9	1.98	0.010	2.6	3.05	0.012	1.9	3.44	0.008	0.9	282
$Palsa_{cop}$	-4.39 ± 1.52	6.3	2.00	0.012	2.0	3.00	0.017	0.6	3.47	0.014	2.1	70
Bog_{cop}	-3.00 ± 0.88	5.4	2.00	0.010	2.3	3.05	0.017	1.4	3.41	0.014	0.7	397

[a]:Energy shift parameter

[b]:path degeneracy (coordination number)

[c]: mean half path length

[d]: Debye-Waller parameter

[e] : normalized sum of squared residuals ($100 \sum_i (data_i\text{-}fit_i)^2/\sum_i data^2$)

[f]: measure of fit accuracy ($((N_{idp}/N_{pts}) \sum_i ((data_i\text{-}fit_i)/\varepsilon_i)^2(N_{idp}\text{-}N_{var})^{-1})$). N_{idp}/N_{pts} and N_{var} are the number of independent points in the model fit (16.3), the total number of data points (329) and the number of fit variables (8), respectively.

note: The passive amplitude reduction factor was set to 0.9 for all models and the Debye-Waller parameters were defined as constants within the ferrihydrite with adsorbed WEOM samples and the coprecipitate samples for the Fe-Fe_1 and Fe-Fe_2 path each. The Debye-Waller parameters were similar to other published values[7,8]. We tried to include a multiple Fe-O-O scattering path, as reported elsewhere[8,9], but this did not change the fitting parameters or goodness of the fit. We also attempted to include an Fe-C path in the coprecipitate spectra, as has been previously fit in Fe-OC coprecipitates with peat OC[7], but the additional path did not match the spectra or significantly improve the fit (F-test).

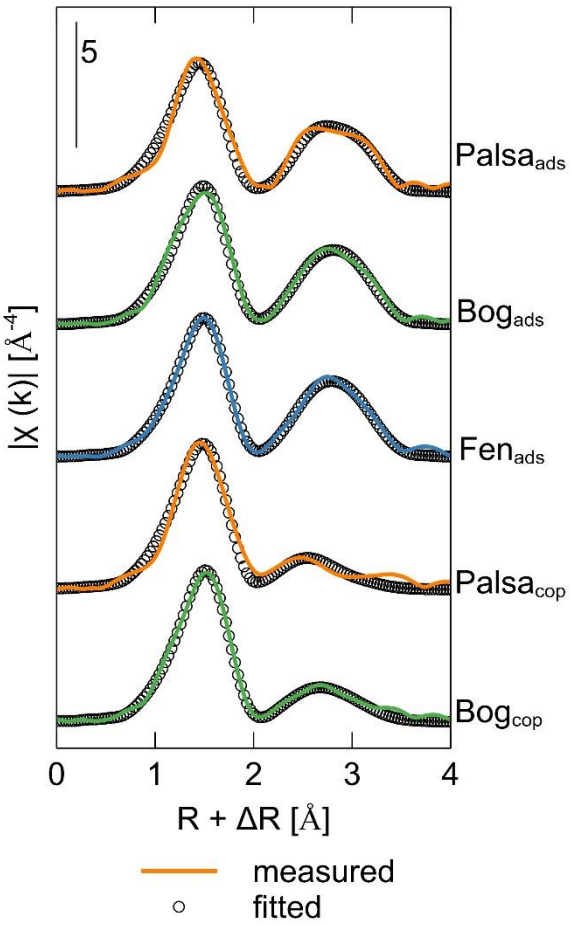

Figure S4: Fe *K*-edge Fourier-transform magnitudes of ferrihydrite with adsorbed WEOM (ads) of palsa, bog and fen, and Fe-OC coprecipitates (cop) synthesized with WEOM from palsa and bog soils. Solid lines show the measured data and open circles represent the fitted model. Fitting parameters are displayed in Table S7.

Text S5: Shell fitting of Fourier-transformed Fe K-edge EXAFS

To elucidate changes in local coordination environment and crystal structure, we conducted shell fitting analysis on the Fourier-transformed Fe *K*-edge EXAFS region. All spectra showed two dominant shells: one at ca. 1.99 Å, corresponding to a single scatter Fe-O path, and one feature ranging from 2.1 to 3.6 Å, which was fit with two single-scatter Fe-Fe paths (Figure S4). The two Fe-Fe paths are defined as edge-sharing Fe-Fe$_1$ (R= 3.00-3.05 Å) and corner-sharing Fe-Fe$_2$ (R=3.41-3.47 Å). Their coordination numbers (CNs) varied depending on OC binding mechanism (adsorption vs coprecipitation) and type of used WEOM (Table S7). All samples of ferrihydrite with adsorbed WEOM had CNs that are typical for ferrihydrite[9–11], with 2.1-2.6 and 1.9 for Fe-Fe$_1$ and Fe-Fe$_2$, respectively. In contrast, CNs of Fe-Fe$_2$ were slightly lower in coprecipitates (0.6 for coprecipitates with palsa WEOM and 1.4 for coprecipitates with bog WEOM). A decrease in corner-sharing Fe-Fe paths due to increased OC content has been described before[11,12] and could indicate lower ferrihydrite particle size[13] and/or lower

crystallinity due to impeded crystal growth in the crystallographic z-axis[14]. However, our CN values cannot be directly compared between adsorption and coprecipitation samples, since Debye-Waller parameters (σ^2) were differently defined in each set, according to the mean values of initially floated σ^2 of samples in each set. The values of σ^2 could be slightly different due to structural ordering differences[7,15]. Within the coprecipitate set, the ones formed with palsa WEOM are likely more poorly crystalline than with bog WEOM, based on CN values of Fe-Fe paths. A higher proportion of carboxylic groups could lead to a lower crystallinity[16].

^{57}Fe Mössbauer spectra and fitting parameters

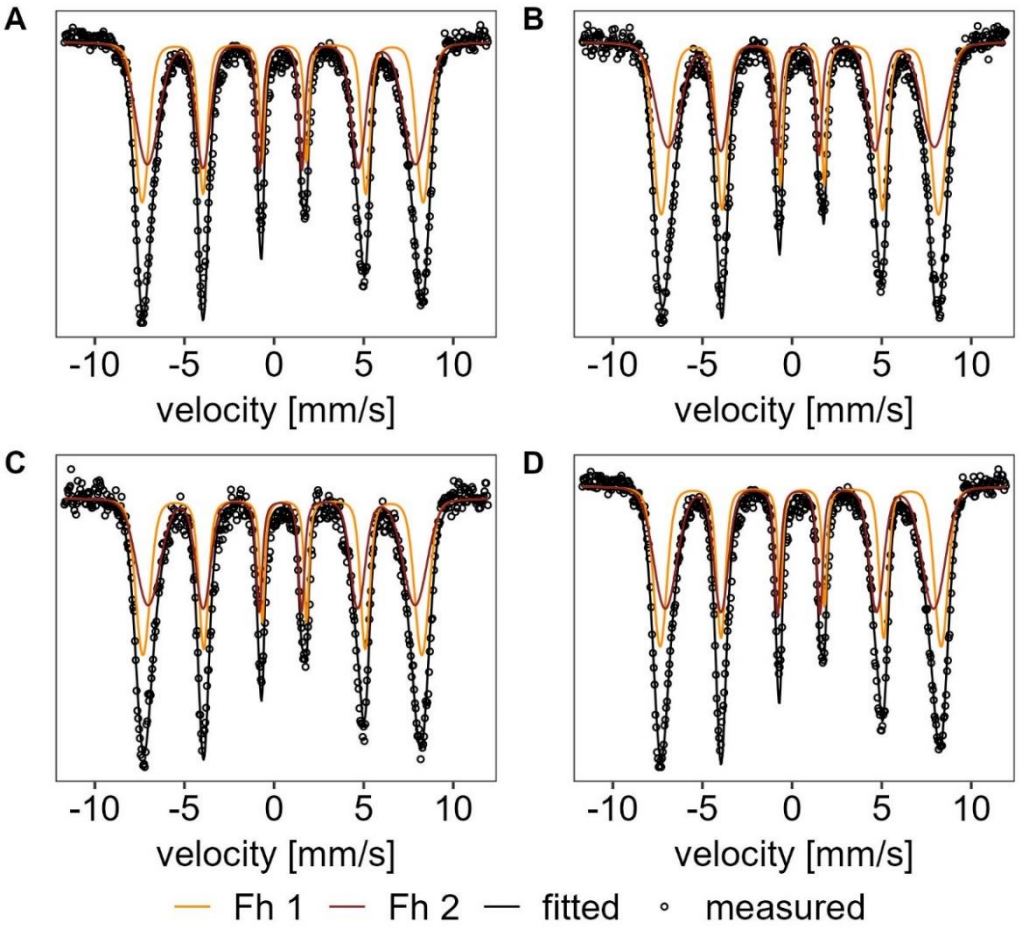

Figure S5: Mössbauer spectra of initial ferrihydrite (A) and with adsorbed WEOM from palsa (B), bog (C) and fen (D), measured at 6 K.

Table S8: Mössbauer parameters of the initial ferrihydrite and after adsorption with WEOM from different permafrost thaw stages. Abbreviations stand for: CS = center shift, QS = quadrupole split, H = hyperfine field, X^2 = goodness of fit parameter. The half width at half maximum was constrained to 0.138 mm s^{-1} during fitting.

Sample	Initial C:Fe [molar]	T [K]	Site	CS [mm/s]	QS [mm/s]	H [T]	Relative area [%]	X^2 [-]
Fh_initial	0	77	Fh	0.45	0.91		100.0	1.04
		6	Fh1	0.55	-0.04	48.95	48.3	2.38
			Fh2	0.34	0.05	47.82	51.7	
Fh_Palsa_ads	2.1	6	Fh1	0.50	-0.07	47.96	51.3	1.12
			Fh2	0.42	0.09	46.07	48.7	
Fh_Bog_ads	1.8	6	Fh1	0.52	-0.06	48.27	48.4	1.04
			Fh2	0.39	0.03	46.18	51.6	
Fh_Fen_ads	1.8	6	Fh1	0.53	-0.05	48.62	44.7	1.95
			Fh2	0.39	0.02	46.42	55.3	

Fourier-transform infrared spectroscopy (FTIR) and peak ratios

Table S9: Assignment of peaks in FTIR spectra (Chen et al.[2], Tfaily et al.[17], Niemeyer et al.[18] and references therein).

wavenumber [cm^{-1}]	assignment
1030, 1050, 1170	C-O and C-OH stretches of carbohydrates
1400	symmetric COO^- stretch
1630	aromatic C=C stretch and/or asymmetric COO^- stretch
1720	C=O stretch in COOH

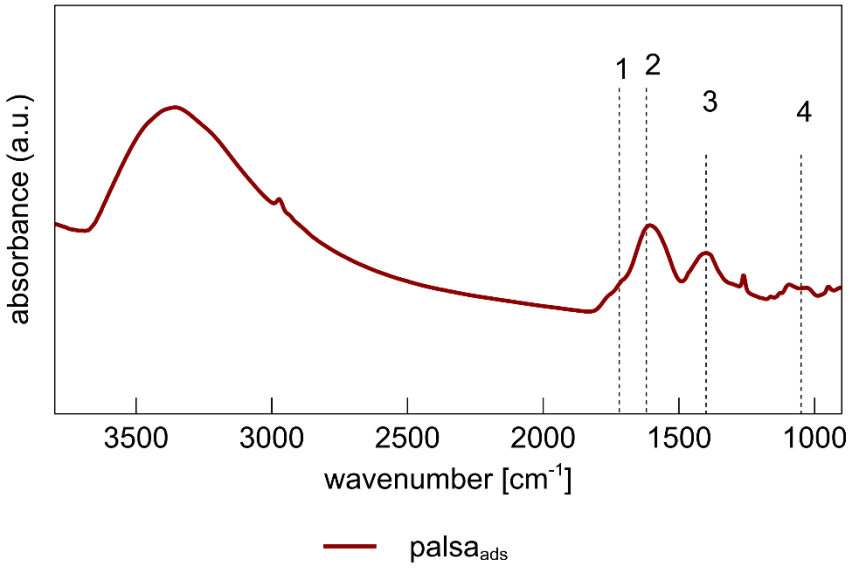

Figure S6: Example of a FTIR spectra from 900-3700 cm^{-1} of solids post-adsorption using WEOM from palsa. Numbers stand for the FTIR bands that were interpreted in the main text: 1 = 1720 cm^{-1} (C=O stretch in COOH), 2 = 1630 cm^{-1} (aromatic C=C stretch and/or asymmetric COO^- stretch), 3 = 1400 cm^{-1} (symmetric COO^- stretch), 4 = 1050 cm^{-1} (C-O stretch of carbohydrates) according to the references given in Table S9.

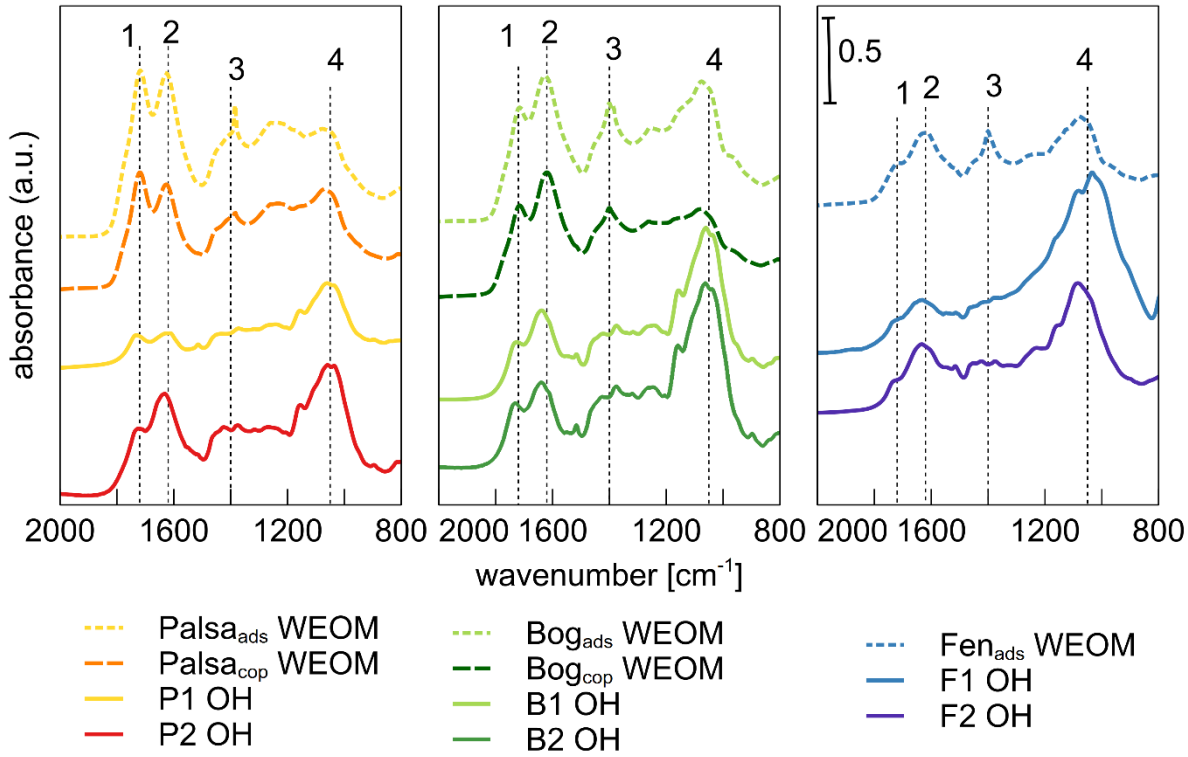

Figure S7: FTIR spectra of the initial WEOM of palsa, bog and fen soils used for adsorption with ferrihydrite (ads) and of palsa and bog soils used for coprecipitation with dissolved Fe(II) (cop) in comparison to solid phase OM from the same soil horizon (OH= organic horizon) of representative soil cores. Numbers stand for the following wavenumbers and functional groups: 1 = 1720 cm^{-1} (C=O stretch in COOH), 2 = 1630 cm^{-1} (aromatic C=C stretch and/or asymmetric COO- stretch), 3 = 1400 cm^{-1} (symmetric COO- stretch), 4 = 1050 cm^{-1} (C-O stretch of carbohydrates).

Table S10: Peak ratios (PR) of initial WEOM of palsa, bog and fen soils (before binding) and of WEOM bound to ferrihydrite or in Fe-OC coprecipitates (after binding). Values are based on peak height after normalization of FTIR spectra.

type of PR		adsorption			coprecipitation	
		palsa	bog	fen	palsa	bog
1630 cm^{-1}/1050 cm^{-1}	before binding	1.5	1.1	0.9	1.0	1.3
(aromatic C=C/ C-O	after binding	3.4	2.7	1.0	1.6	1.2
in carbohydrates)	% change	128.3	151.0	17.8	50.3	-4.7
1400 cm^{-1}/1050 cm^{-1}	before binding	1.0	0.9	0.8	0.8	0.8
(COO^- stretch/ C-O	after binding	2.5	1.8	1.0	1.1	0.8
in carbohydrates)	% change	156.6	100.5	25.7	32.9	3.0

FT-ICR-MS data and intensity-weighted parameters

Table S11: Number of total assigned formulae, N-containing and S-containing formulae as well as (relative intensity weighted,) average parameters across all assigned molecular formulae of measured samples by FT-ICR-MS. Samples include dissolved WEOM from palsa, bog and fen before binding and after binding (by adsorption to ferrihydrite or coprecipitation with dissolved Fe(II)). Abbreviations stand for DBE/C_w= weighted double bond equivalent per number of C atoms in a detected molecule, NOSC= non-weighted nominal oxidation state of organic carbon, $NOSC_w$ = weighted nominal oxidation state of organic carbon, ΔG_{ox}^0= standard molar Gibbs free energy of oxidation half reaction (calculated from unweighted NOSC values), $modAI_w$= weighted modified aromaticity index according to Koch & Dittmar (2006).

		adsorption			coprecipitation	
		Palsa	Bog	Fen	Palsa	Bog
Total number of assigned formulae	before binding	3304	3099	3003	3475	3594
	after binding	3253	3045	1918	3667	3650
Number of N-containing molecular formulae	before binding	1118	840	816	1079	1246
	after binding	1152	1125	594	1174	1376
Number of S-containing molecular formulae	before binding	69	60	143	60	66
	after binding	103	217	145	217	179
Molecular $mass_w$ [Da]	before binding	449	376	359	431	428
	after binding	405	333	318	404	353
DBE/C_w	before binding	0.55	0.54	0.56	0.50	0.58
	after binding	0.46	0.42	0.47	0.45	0.50
NOSC	before binding	0.04	0.05	0.02	-0.05	0.07
	after binding	-0.08	-0.22	-0.20	-0.10	-0.07
$NOSC_w$	before binding	-0.01	-0.01	0.02	-0.16	0.14
	after binding	-0.31	-0.45	-0.32	-0.31	-0.16
ΔG_{ox}^0 [kJ mol^{-1} C^{-1}]	before binding	59.3	58.8	59.6	61.6	58.3
	after binding	62.6	66.6	65.9	63.3	62.3
$modAI_w$	before binding	0.39	0.36	0.40	0.33	0.41
	after binding	0.30	0.23	0.30	0.28	0.32

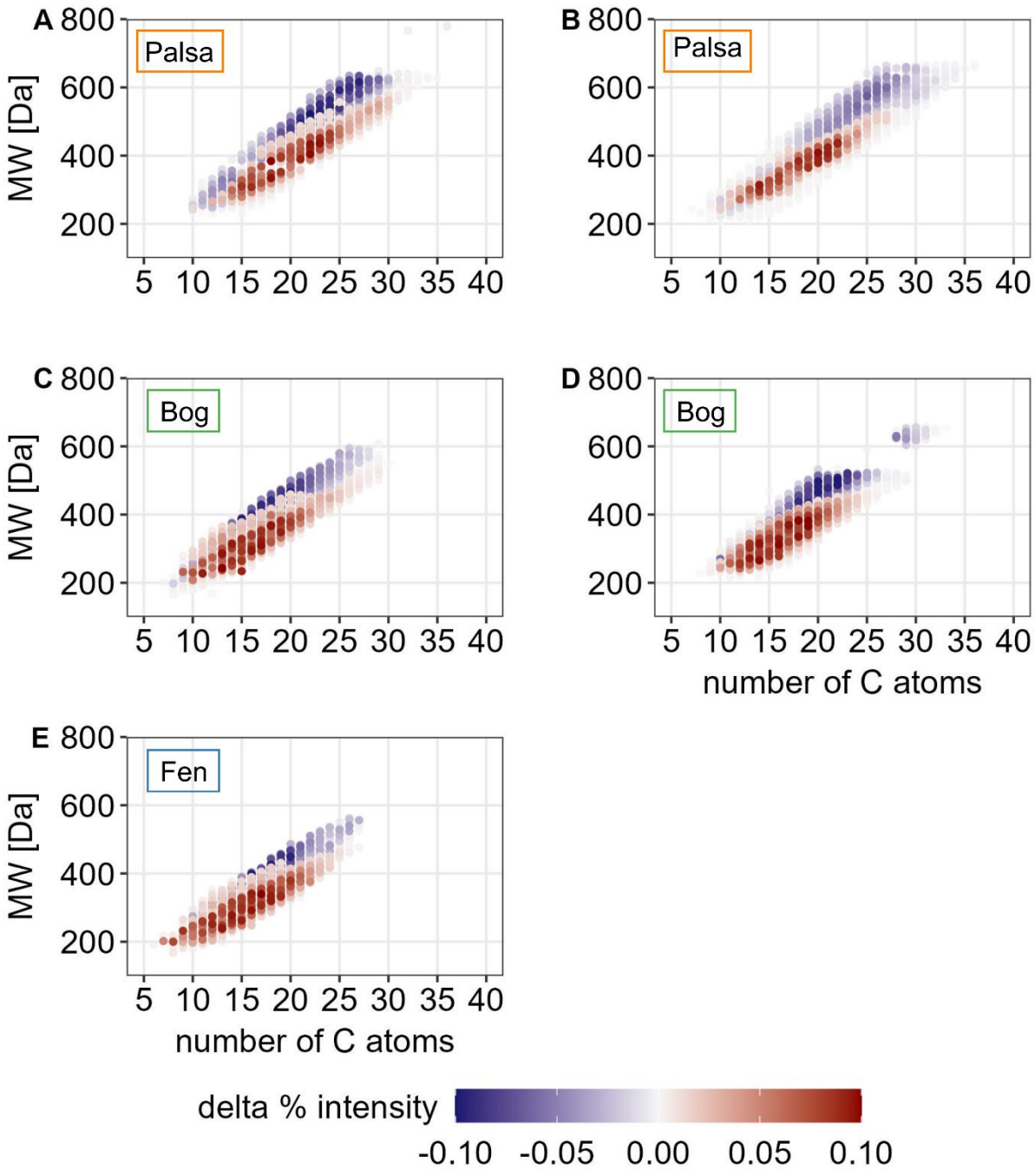

Figure S8: Molecular weight against number of C atoms in a detected molecule before and after adsorption of ferrihydrite with WEOM of palsa (A), bog (C), and fen (E), and coprecipitation of dissolved Fe(II) with WEOM (B, D) from palsa (B) and bog (D) soils. Organic matter compounds which are lost from the dissolved phase, i.e., preferentially bound during adsorption or coprecipitation, are displayed in blue and those retained in solution in red.

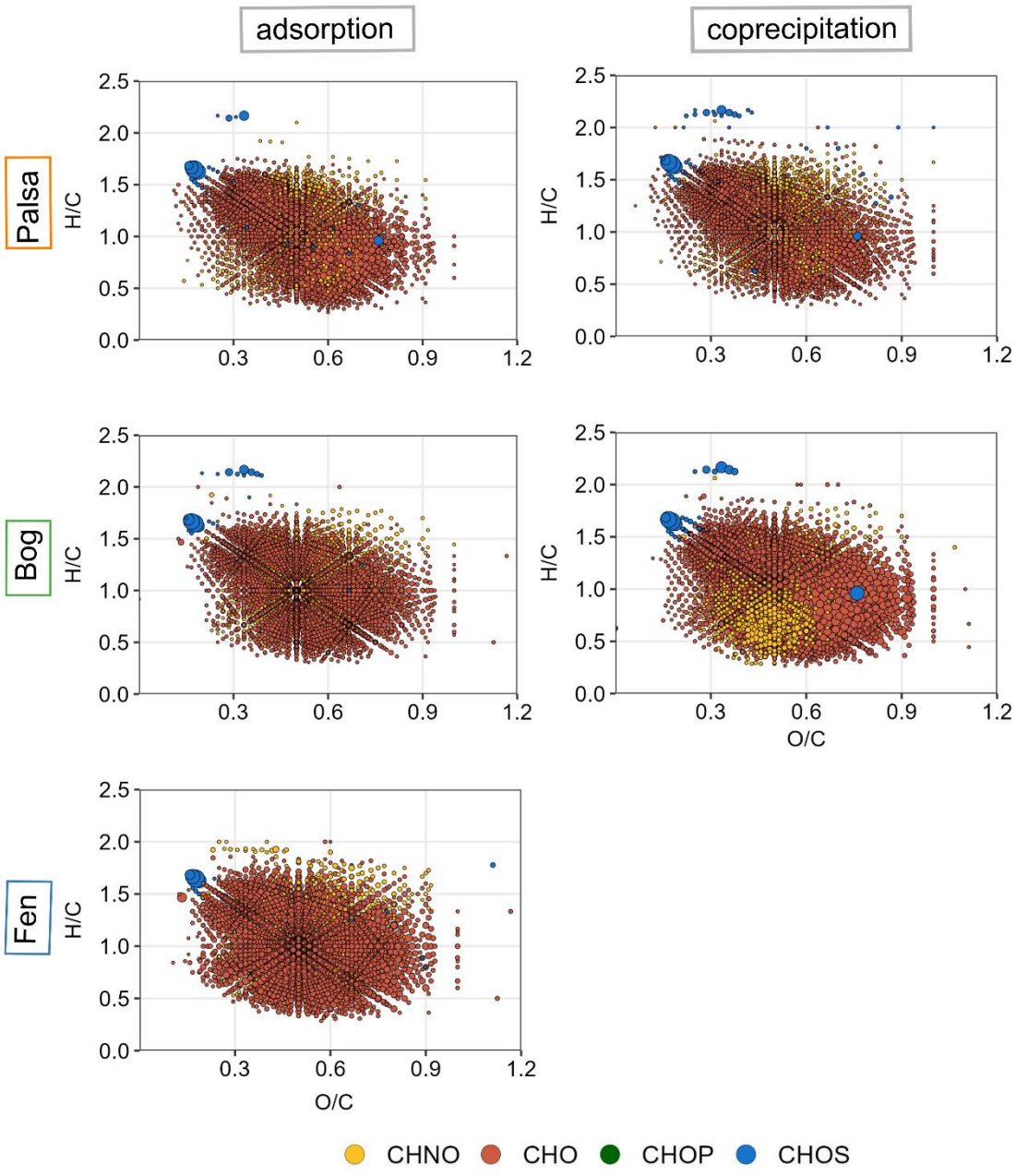

Figure S9: Initial composition of water-extractable organic matter from each experiment, displaying Van Krevelen diagrams (H/C against O/C) of each OC compound. The size of each circle represents the relative intensity of the given OC compound and the colour indicates the elemental composition.

Specific ultraviolet absorption (254 nm) data

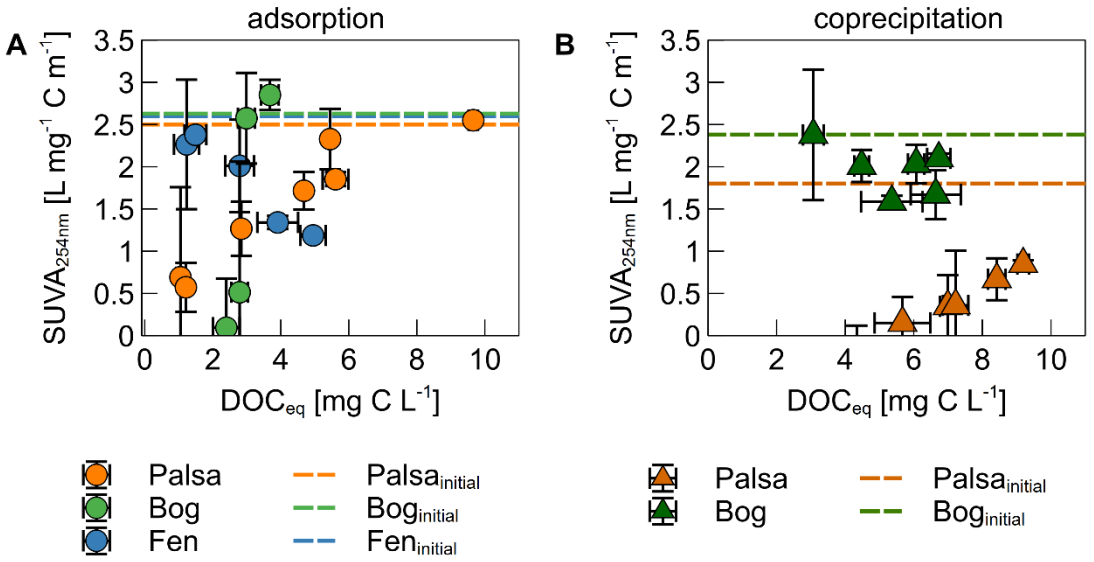

Figure S10: Specific ultraviolet absorption ($SUVA_{254}$) measured at 254 nm of WEOM from palsa, bog and fen soils after adsorption to ferrihydrite (A) or coprecipitation of dissolved Fe(II) with WEOM from palsa and bog soils (B) against the dissolved organic carbon in equilibrium. The SUVA value of the initial WEOM is displayed as a dotted line for each experiment. Some absolute absorption values were below detection limit (e.g. for bog adsorption experiment) and are thus not included in the graph. All data points and error bars represent the average and standard deviation of experimental triplicates, respectively.

References

(1) Lagarec, K.; Rancourt, D. G. Extended Voigt-based analytic lineshape method for determining N-dimensional correlated hyperfine parameter distributions in Mössbauer spectroscopy. *Nuclear Instruments and Methods in Physics Research Section B: Beam Interactions with Materials and Atoms* **1997**, *129* (2), 266–280. DOI: 10.1016/s0168-583x(97)00284-x.

(2) Chen, C.; Dynes, J. J.; Wang, J.; Sparks, D. L. Properties of Fe-organic matter associations via coprecipitation versus adsorption. *Environmental science & technology* **2014**, *48* (23), 13751–13759. DOI: 10.1021/es503669u. Published Online: Nov. 12, 2014.

(3) Brunauer, S.; Emmett, P. H.; Teller, E. Adsorption of Gases in Multimolecular Layers. *J. Am. Chem. Soc.* **1938**, *60* (2), 309–319. DOI: 10.1021/ja01269a023.

(4) Cornell, R. M.; Schwertmann, U. *The iron oxides*, 2., completely rev. and extended ed.; Wiley-VCH, 2003. DOI: 10.1002/3527602097.

(5) Ravel, B.; Newville, M. ATHENA and ARTEMIS Interactive Graphical Data Analysisusing IFEFFIT. *Phys. Scr.* **2005**, *2005* (T115), 1007. DOI: 10.1238/Physica.Topical.115a01007.

(6) Kaur, N.; Gräfe, M.; Singh, B.; Kennedy, B. Simultaneous Incorporation of Cr, Zn, Cd, and Pb in the Goethite Structure. *Clays and Clay Minerals* **2009**, *57* (2), 234–250. DOI: 10.1346/CCMN.2009.0570210.

(7) Chen, K.-Y.; Chen, T.-Y.; Chan, Y.-T.; Cheng, C.-Y.; Tzou, Y.-M.; Liu, Y.-T.; Teah, H.-Y. Stabilization of Natural Organic Matter by Short-Range-Order Iron Hydroxides. *Environ. Sci. Technol.* **2016**, *50* (23), 12612–12620. DOI: 10.1021/acs.est.6b02793. Published Online: Nov. 16, 2016.

(8) ThomasArrigo, L. K.; Notini, L.; Shuster, J.; Nydegger, T.; Vontobel, S.; Fischer, S.; Kappler, A.; Kretzschmar, R. Mineral characterization and composition of Fe-rich flocs from wetlands of Iceland: Implications for Fe, C and trace element export. *The Science of the total environment* **2022**, *816*, 151567. DOI: 10.1016/j.scitotenv.2021.151567. Published Online: Nov. 8, 2021.

(9) Mikutta, C. X-ray absorption spectroscopy study on the effect of hydroxybenzoic acids on the formation and structure of ferrihydrite. *Geochimica et Cosmochimica Acta* **2011**, *75* (18), 5122–5139. DOI: 10.1016/j.gca.2011.06.002.

(10) Waychunas, G.; Rea, B.; Fuller, C.; Davis, J. Surface chemistry of ferrihydrite: Part 1. EXAFS studies of the geometry of coprecipitated and adsorbed arsenate. *Geochimica et Cosmochimica Acta* **1993**, *57* (10), 2251–2269. DOI: 10.1016/0016-7037(93)90567-G.

(11) ThomasArrigo, L. K.; Kaegi, R.; Kretzschmar, R. Ferrihydrite Growth and Transformation in the Presence of Ferrous Iron and Model Organic Ligands. *Environ. Sci. Technol.* **2019**, *53* (23), 13636–13647. DOI: 10.1021/acs.est.9b03952. Published Online: Nov. 13, 2019.

(12) Mikutta, C.; Mikutta, R.; Bonneville, S.; Wagner, F.; Voegelin, A.; Christl, I.; Kretzschmar, R. Synthetic coprecipitates of exopolysaccharides and ferrihydrite. Part I: Characterization. *Geochimica et Cosmochimica Acta* **2008**, *72* (4), 1111–1127. DOI: 10.1016/j.gca.2007.11.035.

(13) Mikutta, C.; Frommer, J.; Voegelin, A.; Kaegi, R.; Kretzschmar, R. Effect of citrate on the local Fe coordination in ferrihydrite, arsenate binding, and ternary arsenate complex formation. *Geochimica et Cosmochimica Acta* **2010**, *74* (19), 5574–5592. DOI: 10.1016/j.gca.2010.06.024.

(14) Michel, F. M.; Ehm, L.; Antao, S. M.; Lee, P. L.; Chupas, P. J.; Liu, G.; Strongin, D. R.; Schoonen, M. A. A.; Phillips, B. L.; Parise, J. B. The structure of ferrihydrite, a nanocrystalline material. *Science (New York, N.Y.)* **2007**, *316* (5832), 1726–1729. DOI: 10.1126/science.1142525. Published Online: May. 24, 2007.

(15) Karlsson, T.; Persson, P. Coordination chemistry and hydrolysis of Fe(III) in a peat humic acid studied by X-ray absorption spectroscopy. *Geochimica et Cosmochimica Acta* **2010**, *74* (1), 30–40. DOI: 10.1016/j.gca.2009.09.023.

(16) Curti, L.; Moore, O. W.; Babakhani, P.; Xiao, K.-Q.; Woulds, C.; Bray, A. W.; Fisher, B. J.; Kazemian, M.; Kaulich, B.; Peacock, C. L. Carboxyl-richness controls organic carbon preservation during coprecipitation with iron (oxyhydr)oxides in the natural environment. *Commun Earth Environ* **2021**, *2* (1), 1–13. DOI: 10.1038/s43247-021-00301-9.

(17) Tfaily, M. M.; Cooper, W. T.; Kostka, J. E.; Chanton, P. R.; Schadt, C. W.; Hanson, P. J.; Iversen, C. M.; Chanton, J. P. Organic matter transformation in the peat column at Marcell Experimental Forest: Humification and vertical stratification. *J. Geophys. Res. Biogeosci.* **2014**, *119* (4), 661–675. DOI: 10.1002/2013JG002492.

(18) Niemeyer, J.; Chen, Y.; Bollag, J.-M. Characterization of Humic Acids, Composts, and Peat by Diffuse Reflectance Fourier-Transform Infrared Spectroscopy. *Soil Science Society of America Journal* **1992**, *56* (1), 135–140. DOI: 10.2136/sssaj1992.03615995005600010021x.